Since January 2020 Elsevier has created a COVID-19 resource centre with free information in English and Mandarin on the novel coronavirus COVID-19. The COVID-19 resource centre is hosted on Elsevier Connect, the company's public news and information website.

Journal of Pharmacological Sciences 128 (2015) 159–169

HOSTED BY

Contents lists available at ScienceDirect

Journal of Pharmacological Sciences

journal homepage: www.elsevier.com/locate/jphs

Full paper

In vitro anti-reovirus activity of kuraridin isolated from *Sophora flavescens* against viral replication and hemagglutination

Hyung-Jun Kwon [a, 1], Jae-Ho Jeong [b, 1], Seung Woong Lee [c], Young Bae Ryu [a], Hyung Jae Jeong [a], Kyungsook Jung [a], Jae Sung Lim [d], Kyoung-Oh Cho [e], Woo Song Lee [a], Mun-Chual Rho [a, **], Su-Jin Park [a, *]

[a] *Eco-friendly Bio-material Research Center, Korea Research Institute of Bioscience and Biotechnology, 181 Ipsin-gil, Jeongeup-si, Jeonbuk 580-185, Republic of Korea*
[b] *Department of Microbiology, Chonnam National University Medical School, Gwangju 501-746, Republic of Korea*
[c] *Department of Chemistry, Mokwon University, Daejeon 302-729, Republic of Korea*
[d] *Department of Biochemistry, Chonnam National University Medical School, Gwangju, Republic of Korea*
[e] *Biotherapy Human Resources Center, College of Veterinary Medicine, Chonnam National University, Gwangju 500-757, Republic of Korea*

ARTICLE INFO

Article history:
Received 12 December 2014
Received in revised form
5 April 2015
Accepted 21 April 2015
Available online 30 April 2015

Keywords:
Anti-reovirus activity
Sophora flavescens
Kuraridin
Viral absorption and replication
Hemagglutination

ABSTRACT

In this study, we evaluated the anti-reovirus activity of kuraridin isolated from the roots of *Sophora flavescens*. In particular, we focused on whether this property is attributable to direct inhibition of reovirus attachment and/or inhibition of viral replication with the aid of time-of-addition (pre-treatment, simultaneous treatment, and post-treatment) experiments. No significant antiviral activity of kuraridin was detected in the pre-treatment assay. In the simultaneous assay, the 50% effective inhibitory concentrations (EC_{50}) of kuraridin were 15.3–176.9 μM against human type 1–3 reoviruses (HRV1–3) and Korean porcine reovirus (PRV). Kuraridin completely blocked binding of viral sigma 1 protein to sialic acids at concentrations lower than 82.5 μM in the hemagglutination inhibition assay. Moreover, kuraridin inhibited HRV1–3 and PRV viral replication with EC_{50} values of 14.0–62.0 μM. Quantitative real-time PCR analysis disclosed strong suppression of reovirus RNA synthesis at the late stage (18 h) of virus replication by kuraridin. The viral yields of kuraridin-treated cells were significantly reduced at 24 h post-infection, compared with DMSO-treated cells. Our results collectively suggest that kuraridin inhibits virus adsorption and replication by inhibiting hemagglutination, viral RNA and protein synthesis and virus shedding, supporting its utility as a viable candidate antiviral drug against reoviruses.

1. Introduction

Mammalian reovirus (MRV) is the prototype member of the *Reoviridae* family of non-enveloped double-stranded RNA (dsRNA) viruses, with a genome composed of ten segments. Reoviruses, originally referred to as “respiratory enteric orphans”, were first isolated from humans in the United States and Mexico in the 1950s (1). MRVs are represented by four prototype strains: type 1 Lang (T1L), type 2 Jones (T2J), type 3 Dearing (T3D) and type 4 Ndelle (T4N), with the majority of strains assigned to serogroups T1L, T2J or T3D (2). Reoviruses have been isolated from the respiratory and enteric tracts of children with mild respiratory or gastrointestinal symptoms (1). However, limited studies have focused on human reovirus-associated neurological disease to date (3). Pneumonia and other respiratory diseases in both naturally and experimentally infected primates (4), and isolation of reoviruses from children with meningitis and encephalitis are widely documented (5, 6).

MRVs infect a wide range of hosts, including livestock (pig, cattle and chickens), contributing to severe economic losses worldwide. The use of antiviral agents is not commonplace because of their toxicity and high production costs. Hence, effective and inexpensive alternatives to antiviral drugs remain an urgent unmet medical need (7). Many traditional medicinal plants display strong antiviral

* Corresponding author. Tel.: +82 63 570 5240; fax: +82 63 570 5239.
** Corresponding author. Tel.: +82 63 570 5230; fax: +82 63 570 5239.
E-mail addresses: rho-m@kribb.re.kr (M.-C. Rho), sjpark@kribb.re.kr (S.-J. Park).
Peer review under responsibility of Japanese Pharmacological Society.
[1] Both authors contributed equally to the work and should be considered as first authors.

http://dx.doi.org/10.1016/j.jphs.2015.04.007

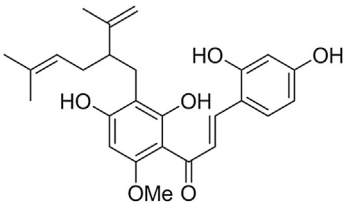

Fig. 1. The structure of kuraridin.

activities, and their utility in the successful treatment of infected animals and humans has been demonstrated (8, 9).

The life cycle of viruses is divided into several stages, including cell surface attachment, penetration, uncoating, replication (protein synthesis) and release, all of which provide targets for antiviral agents (9). Currently, more than 40 antiviral drugs are licensed for the treatment of human immunodeficiency virus (HIV), hepatitis B virus (HBV) and herpesviruses. However, the number of licensed antiviral drugs for treatment of highly pathogenic RNA virus infections remains limited (10). These viral diseases are considered difficult to treat with selective antiviral chemotherapy, highlighting the need for further refinement of antiviral drug design and development. Medicinal plants have a variety of chemical constituents, including alkaloids, tannins, saponins, flavonoids, terpenoids, lignans and coumarins, known to inhibit the replication cycles of various DNA and RNA virus types. Compounds derived from natural sources are therefore of significant interest as possible sources of viral infection control (7–9).

Dried roots of *Sophora flavescens* Ait. (*S. flavescens*) have been historically used in traditional Chinese herbal medicine, owing their anti-inflammatory, antiarrhythmic, antipyretic, antiasthmatic, and antiulcerative effects, and for the treatment of diarrhea, gastrointestinal hemorrhage, and eczema (11). Additionally, a formulation containing *S. flavescens* is reported to inhibit angiogenesis in a collagen-induced arthritis rat model (12). In previous studies, quinolizidine alkaloids, flavonoids, and triterpenoids were isolated from the roots of *S. flavescens* (13). Recently, quinolizidine alkaloids and flavonoids have been shown to exhibit a wide spectrum of pharmacological activities, including anticancer, anti-inflammatory, antitumor, cardioprotective, neuroprotective, antibacterial, and anti-influenza properties (11,13–21). However, the potential anti-reovirus activities of extracts and compounds isolated from *S. flavescens* have not been examined to date. In the current investigation, we evaluated the abilities of the MeOH extract, EtOAc fraction and kuraridin isolated from *S. flavescens* to inhibit human type 1–3 reoviruses (HRV1–3) and Korean porcine reovirus (PRV). Antiviral assays were employed to determine whether the *S. flavescens* compounds alter reovirus activity by inhibiting virus attachment and/or replication.

2. Materials and methods

2.1. Analytical equipment

The ^{1}H NMR (400 MHz) and ^{13}C NMR (100 MHz) spectra were obtained on JEOL ECS400 spectrometer, with CD_3OD as a solvent. The ESI-MS was determined using an Agilent 6430 LC/MS/MS and 1100 LC/MS spectrometer. Reversed-phase CC was carried out using RP-C18 silica gel (Cosmosil 140C18-PREP, 140 μm, Nacalai tesque, INC.). Silica gel CC was conducted using Kieselgel 60 (70–230 and 230–400 mesh, Merck). TLC was conducted using Kieselgel 60 F254 plates (Merck).

2.2. Extract and isolation

The *S. flavescens* were purchased at an herbal market in Jeongeup, Korea. A voucher specimen (PB-012–012) has been deposited in the Korea Plant Extract Bank, Korea Research Institute of Bioscience and Biotechnology. Dried roots of *S. flavescens* (5 kg) were extracted with MeOH (10 L) for 7 days at room temperature. The MeOH extract was evaporated *in vacuo*, yielding a residue (193 g). The residue was suspended in distilled water (1 L) and extracted with *n*-hexane, $CHCl_3$, EtOAc and BuOH. In this process, *n*-hexane (3.9 g), $CHCl_3$ (22 g), EtOAc (33.5 g) and BuOH (38.9 g) layers were obtained respectively. The EtOAc layer was submitted to open column chromatography on silica gel (230–400 mesh, 300 g,

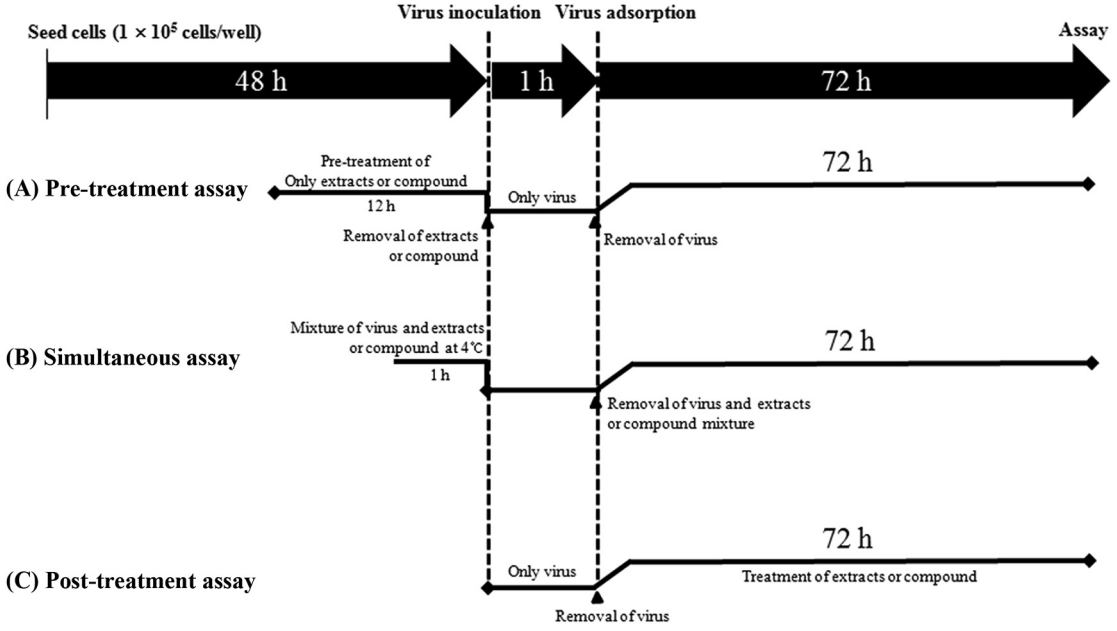

Fig. 2. Antiviral assay strategies at different stages of virus infection. (A) Pre-treatment assay: addition of the MeOH extract, EtOAc fraction or kuraridin at 12 h prior to virus infection, (B) Simultaneous treatment assay: virus incubated with the MeOH extract, EtOAc fraction or kuraridin isolated from *S. flavescens* at 4 °C for 1 h, (C) Post-treatment assay: addition of the MeOH extract, EtOAc fraction or kuraridin at 1 h post-viral infection.

Merck) using gradient solvent system $CHCl_3$-EtOAc (100:1, 80:1, 50:1, 30:1, 10:1, 1:1, 1:10, 1:100; v/v, each 1L) as eluent to yield 21 fractions (F1–F21) by TLC profile. F15 (2 g) was subjected to column chromatography on ODS (70 g, Cosmosil 140C18-PREP, 140 μm, Nacalai tesque, INC.) eluted with MeOH–H_2O (50:50, 60:40, 70:30, 80:20, 90:10, 100:0; v/v, each 200 mL) to yielded 12 fractions (F15–1~12) based on the TLC profile. F15–9 (120 mg) was chromatographed on reverse-phase (10 g) column using a MeOH–H_2O solvent gradient (70:30, 80:20, 90:10, 100:0; v/v, each 50 mL) to yield compound **1** (53 mg). Compound **1** was obtained as orange oil, it exhibited a molecular ion peak at *m/z* 438 $[M+H]^+$ in the ESI-MS and molecular formula was determined as $C_{26}H_{30}O_6$. The presence of lavandulyl group was inferred from three methyl protons [δ 1.55 (3H, s, H-6″), 1.62 (3H, s, H-7″), 1.70 (3H, s, H-10″)], three olefinic protons [δ 5.03 (1H, m, H-4″), 4.58 (1H, br s, H-9″a), 4.53 (1H, br s, H-9″b)], two methylene protons [δ 2.53 (1H, m, H-2″), 2.06 (2H, m, H-3″)] and a multiple at δ 2.61 (2H, m, H-1″). The ^{13}C NMR spectrum revealed the presence of 26 carbons as one carbonyl group, three methylene carbons, four methyl carbons, eight methines and ten quaternary carbons. Thus, the structure of compound **1** was determined by spectroscopic analysis (MS and NMR) and compared with the data published in the literature (22). The compound identified was **kuraridin** (Fig. 1).

***Kuraridin*:** Orange oil. $C_{26}H_{30}O_6$. ESI-MS *m/z*: 439.5 $[M+H]^+$. ^1H NMR (400 MHz, CD_3OD): δ 7.95 (1H, d, *J* = 15.6 Hz, H-2), 7.88 (1H, d, *J* = 15.6 Hz, H-3), 7.39 (1H, d, *J* = 8.9 Hz, H-6′), 6.34 (1H, d, *J* = 2.4 Hz, H-3′), 6.32 (1H, dd, *J* = 8.9, 2.4 Hz, H-5′), 5.99 (1H, s, H-6), 5.03 (1H, m, H-4″), 4.58 (1H, br s, H-9″a), 4.53 (1H, br s, H-9″b), 3.87 (3H, s, OCH_3), 2.61 (2H, m, H-1″), 2.53 (1H, m, H-2″), 2.06 (2H, m, H-3″), 1.70 (3H, s, H-10″), 1.62 (3H, s, H-7″), 1.55 (3H, s, H-6″). ^{13}C NMR (100 MHz, CD_3OD): δ 194.7 (C-4), 165.2 (C-5), 163.9 (C-7), 162.3 (C-9), 162.1 (C-4′), 160.2 (C-2′), 149.7 (C-8″), 139.7 (C-2), 131.7 (C-5″), 131.5 (C-6′), 125.3 (C-4″), 125.0 (C-3), 116.2 (C-1′), 111.1 (C-9″), 108.8 (C-8), 108.7 (C-5′), 106.4 (C-10), 103.5 (C-3′), 91.4 (C-6), 56.0 (OCH_3), 48.7 (C-2″), 32.3 (C-3″), 28.1 (C-1″), 25.9 (C-6″), 19.0 (C-10″), 17.8 (C-7″).

2.3. Cells and viruses

Fetal rhesus monkey kidney (TF-104) cells were grown in Eagle's minimum essential medium (EMEM) supplemented with 5% fetal bovine serum (FBS) and 100 U/mL penicillin, and 100 μg/mL streptomycin and 100 U/mL amphotericin B. Cells were maintained

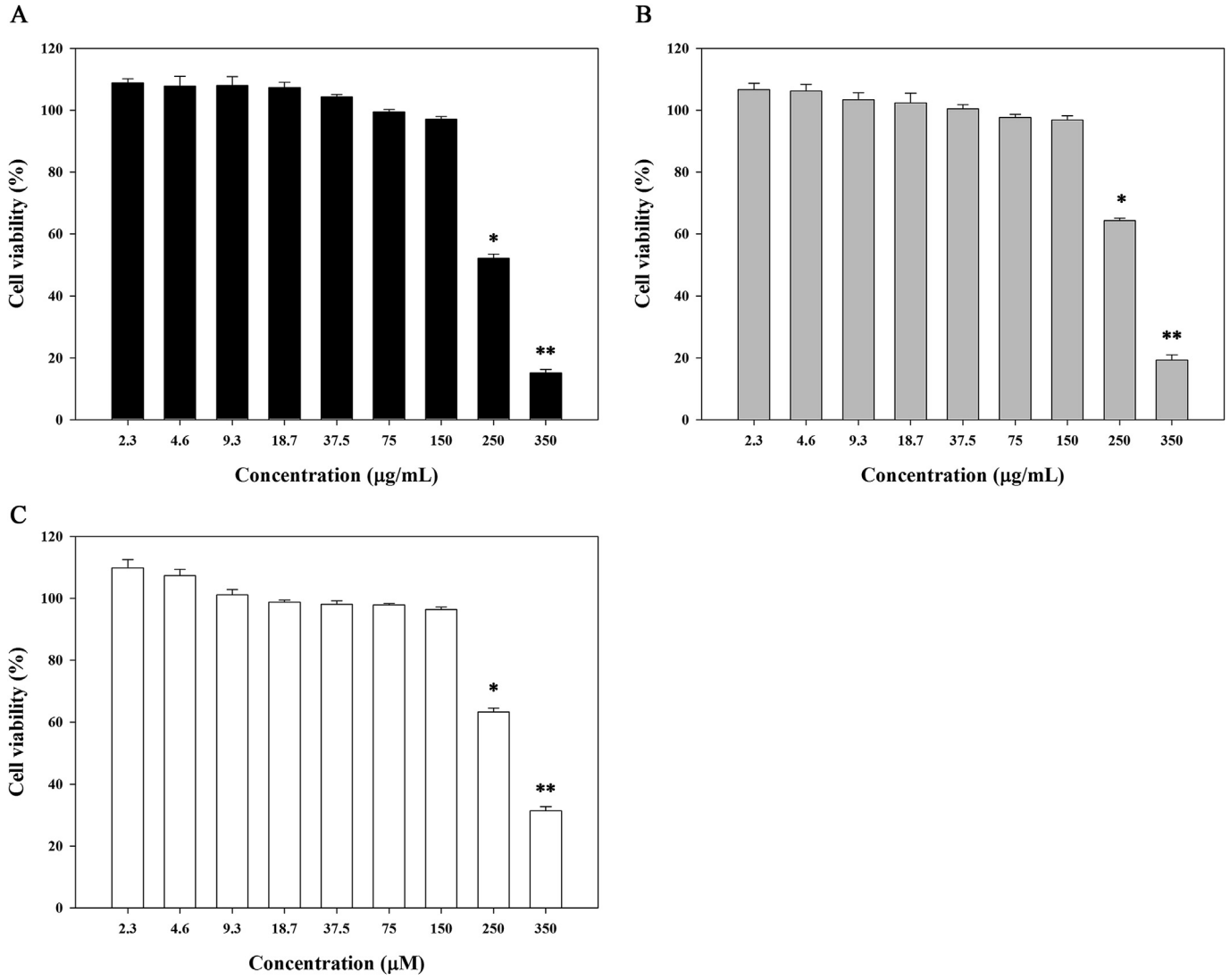

Fig. 3. Cytotoxicity of the MeOH extract, EtOAc fraction, and kuraridin isolated from *S. flavescens* on TF-104 cells. TF-104 cells were treated with various concentrations of the MeOH extract, EtOAc fraction (2.3–300 μg/mL) or kuraridin (2.3–300 μM) for 72 h. Cell viability was measured with the MTT assay, with DMSO-treated cells as the control group. Data are expressed as mean ± ANOVA combined standard error of three independent replicates. $^{**}P < 0.01$, $^{*}P < 0.05$, compared to control DMSO-treated cells.

Table 1
Antiviral activities of the MeOH extract, EtOAc fraction, and kuraridin isolated from *S. flavescens* against reovirus for the simultaneous- and post-treatment assay.

Extract or compound		Simultaneous-treatment assay								Post-treatment assay							
		HRV1 (T1L)		HRV2 (T2J)		HRV3 (T3D)		PRV(KRP113)		HRV1 (T1L)		HRV2 (T2J)		HRV3 (T3D)		PRV(KRP113)	
	CC_{50}[a]	EC_{50}[b]	SI[c]	EC_{50}	SI	EC_{50}	SI	EC_{50}	SI	EC_{50}	SI	EC_{50}	SI	EC_{50}	SI	EC_{50}	SI
MeOH extract (μg/mL)	253.3 ± 1.7	192.4 ± 2.1	1.32	197.0 ± 4.7	1.29	86.1 ± 3.1	2.94	110.9 ± 3.7	2.28	112.1 ± 2.7	2.26	78.0 ± 1.8	3.25	15.6 ± 1.6	16.23	16.5 ± 4.6	15.35
EtOAc fraction (μg/mL)	278.4 ± 1.3	94.6 ± 3.3	2.94	195.9 ± 3.0	1.42	46.3 ± 1.8	6.01	65.1 ± 2.9	4.28	81.4 ± 5.1	3.42	26.5 ± 2.5	10.50	13.8 ± 2.9	20.17	15.2 ± 4.0	18.31
Kuraridin (μM)	302.2 ± 1.6	41.1 ± 1.9	7.35	176.9 ± 3.4	1.71	26.7 ± 3.0	11.32	15.3 ± 1.5	19.80	62.0 ± 1.8	4.90	29.4 ± 2.7	10.28	14.4 ± 1.2	20.98	14.0 ± 4.1	21.59

[a] CC_{50}: mean (50%) value of cytotoxic concentration.
[b] EC_{50}: mean (50%) value of effective concentration.
[c] SI: selective index, CC_{50}/EC_{50}.

at 37 °C with 5% CO_2. Antibiotic, trypsin-EDTA, FBS, and EMEM were supplied by Gibco BRL (Grand Island, NY, USA). The reovirus Type 1 (Lang, ATCC VR-230), Type 2 (Jones, ATCC VR-231), Type 3 (Dearing, ATCC VR-824) purchased from American Type Culture Collection (ATCC) and PRV (KRP113 strain) isolated from fecal samples of Korean diarrheic piglets were used in this study. Reoviruses were preactivated with 10 μg/mL trypsin (GIBCO Invitrogen Corporation, CA, USA) for 30 min at 37 °C before being inoculated onto confluent TF-104 cells and infected cells were maintained in the presence of 1 μg/mL trypsin (GIBCO Invitrogen Corporation, CA, USA).

2.4. Cytotoxicity assay

TF-104 cells were grown in 96 well plates at 1×10^5 cells/well for 48 h. The media in plates were replaced with media containing serial diluted the MeOH extract, EtOAc fraction (2.3–350 μg/mL) or kuraridin (2.3–350 μM) and incubated for 24 h or 72 h. The solution was replaced with only media and 5 μL MTT (3–(4,5–dimethyl thiazol–2–yl)–2,5–diphenyltetrazolium bromide, SIGMA) solution was added to each well and incubated at 37 °C for 4 h. After removal of supernatant, 100 μL 0.04 M HCl-isopropanol was added for solubilization of formazan crystals. Absorbance was measured at 540 nm with subtraction of the background measurement at 655 nm using a microplate reader. Cell viability was calculated as a percentage of the total number of 0.5% DMSO-treated control cells. The CC_{50} was calculated as described (23).

2.5. Antiviral assay

The antiviral assays have been previously described (24), and the visualization of these assays was performed by neutral red method as briefly described.

Pre-treatment assay (Fig. 2A): TF-104 cells were grown in 96 well plates at 1×10^5 cells/well for 48 h. Before virus inoculation, non-cytotoxic concentration ($\leq CC_{50}$) of the MeOH extract and EtOAc fraction or kuraridin isolated from *S. flavescens* were added to the cells and incubated for 12 h. Then extracts and compound were removed and the TF-104 cells were washed 2 times with PBS. Reoviruses at a multiplicity of infection (MOI) of 0.01 were inoculated onto the TF-104 cells for 1 h with occasional rocking. The media was removed and replaced by EMEM containing 1 μg/mL trypsin. The cultures were incubated for 72 h at 37 °C under 5% CO_2 atmosphere until the cells in the infected, untreated control well showed complete viral cytopathic effect (CPE) as observed by light microscopy. Each concentration of extracts and compounds was assayed in triplicate.

After 72 h incubation in all antiviral assays, 0.034% neutral red was added to each well and incubated for 2 h at 37 °C in the dark. The neutral red solution was removed and the cells were washed with PBS (pH 7.4). Destaining solution (containing 1% glacial acetic acid, 49% H_2O, and 50% ethanol) was added to each well. The plates were incubated in the dark for 15 min at room temperature. Absorbance was read at 540 nm using a microplate reader. The EC_{50} that is defined as the concentration offering 50% inhibition of viral yield in cells was calculated as described (23).

Simultaneous treatment assay (Fig. 2B): Various concentrations of MeOH extract and EtOAc fraction or kuraridin were mixed with virus at 0.01 MOI and incubated at 4 °C for 1 h. The mixture were inoculated onto near confluent TF-104 cell monolayers (1×10^5 cells/well) for 1 h with occasional rocking. The solution was removed and the media was replaced. The cultures were incubated for 72 h at 37 °C under 5% CO_2 atmosphere until the cells in the infected, untreated control well showed complete viral CPE as observed by light microscopy. Each concentration of extracts or compound was assayed in triplicate.

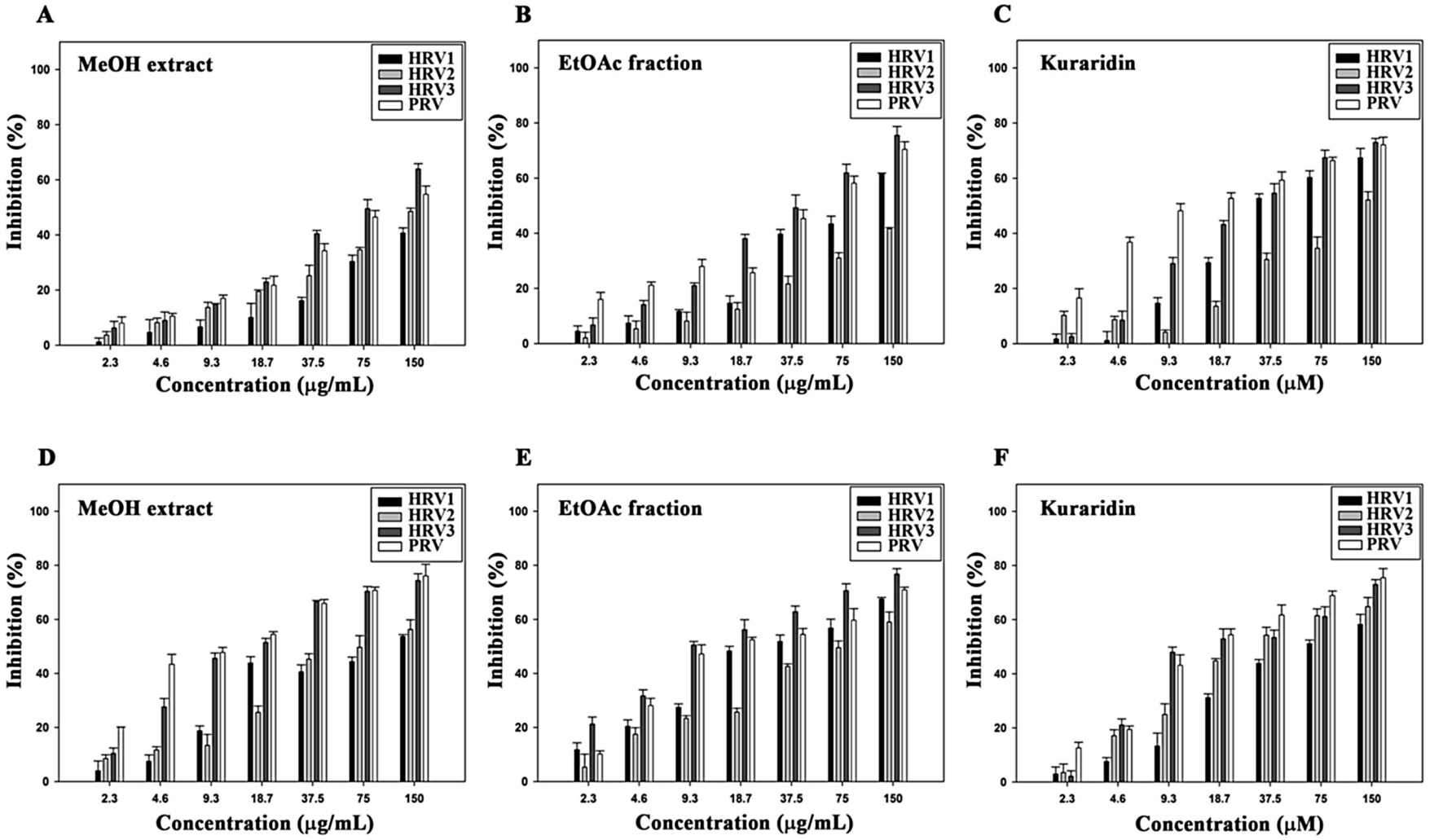

Fig. 4. *In vitro* antiviral activity of the MeOH extract, EtOAc fraction, and kuraridin in simultaneous treatment assay and post treatment assay. (A–C) Simultaneous treatment assay: Reoviruses (HRV1–3 and PRV) infected the TF-104 cells were treated with serial concentrations of the MeOH extract (2.3–150 μg/mL) (A), EtOAc fraction (2.3–150 μg/mL) (B) or kuraridin (2.3–150 μM) (C) at the same time. After 1 h, reoviruses and the extracts and compound were removed and the medium replaced. Cultures were incubated for 72 h at 37 °C under 5% CO_2. (D–F) Post treatment assay: Reoviruses infected TF-104 cells were treated with serial concentration of the MeOH extract (2.3–150 μg/mL) (D), EtOAc fraction (2.3–150 μg/mL) (E) or kuraridin (2.3–150 μM) (F) for 72 h. The *in vitro* antiviral effect was evaluated using the neutral red assay. All assays were performed three times in triplicate. Non-infected and DMSO-treated group was used as the negative control, and reovirus-infected and DMSO-treated group was used as the positive control.

Post treatment assay (Fig. 2C): Reoviruses at 0.01 MOI were inoculated onto near confluent TF-104 cell monolayers (1×10^5 cells/well) for 1 h with occasional rocking. The media was removed and replaced by EMEM with MeOH extract and EtOAc fraction or kuraridin at different concentration. The cultures were incubated for 72 h at 37 °C under 5% CO_2 atmosphere until the cells in the infected, untreated control well showed complete viral CPE as observed by light microscopy. Each concentration of extracts and compound was assayed for virus inhibition in triplicate.

2.6. Hemagglutination inhibition (HI) assay

The hemagglutination inhibition assay was performed to evaluate the effects of the MeOH extract and EtOAc fraction or kuraridin on viral adsorption to target cells. The reoviruses solution (4 HAU/25 μL) was mixed with an equal volume of the extracts or compound (25 μL) in a two-fold serial dilution in PBS (pH 7.4) for 1 h at 4 °C. The prepared solution 50 μL was mixed with an equal volume of 1% human red blood cells (hRBC, type O) in HRV1 or 1% bovine red blood cell (bRBC) in HRV2-3 and PRV suspension and incubated for 1 h at room temperature (25, 26).

2.7. Reverse transcription and quantitative real-time PCR

TF-104 cells were grown to about 90% confluence, infected with HRV1–3 and PRV strain at 0.01 MOI, and cultured in the presence of kuraridin (30 μM) for 6 h or 18 h. For dose-dependant inhibition, TF-104 cells infected with PRV strain at 0.01 MOI were maintained with kuraridin at different concentration (5–50 μM) for 24 h. After incubation, medium was removed. The cells were scraped off, washed twice with PBS, and collected by centrifugation (500 g for 3 min). In order to determine the mRNA expression level of Large 1 (L1) gene of reoviruses, total RNA was isolated using Qiagen RNeasy mini kit (QIAGEN) according to manufacturer's instruction. The primer sequences used for quantitative real-time PCR of viral RNA were 5′- GTG GCA GCG GTG GAT ACG -3' (sense) and Reverse: Reverse: 5′- GCC CTC TGA TGA CAA GAT GGA -3' (antisense) (27). The total RNA was reverse transcribed into cDNA using the High Capacity RNA-to-cDNA master mix (Applied Biosystems) according to the manufacturer's instruction. Reverse transcription was performed at 42 °C for 1 h. The enzyme was inactivated at 95 °C for 5 min. The cDNA was stored at −20 °C or directly used in quantitative real-time PCR. Real-time PCR was conducted using 2 μL of cDNA and Power SYBR Green PCR 2X master mix (Applied Biosystems). Cycling conditions for real-time PCR were as follows: 95 °C for 1 min, followed by 40 cycles of 95 °C for 15 s and 60 °C for 15 s. Real-time PCR was conducted using the Step One Plus Real-time PCR system, and the data were analyzed with StepOne software v2.1 (Applied Biosystems).

2.8. Confocal fluorescence imaging

TF-104 cells were grown on 8-well chamber slides (LAB-TEK, NUNC, USA), and the monolayers were infected with PRV at 1 MOI for 1 h. The TF-104 cells were removed the virus solution and replaced by EMEM with kuraridin (30 μM) under test. The cells were cultured for 24 h at 37 °C in a 5% CO_2 atmosphere, washed three times with PBS (pH 7.4), and fixed in 4% paraformaldehyde solution for 15 min at room temperature. After three times washed with PBS (pH 7.4), cells were incubated at 37 °C for 1 h with sigma 1 (s1)-specific monoclonal antibody against reovirus (Abcam, MA, USA) diluted 1:50 in PBS (pH 7.4). After washing with PBS (pH 7.4), cells were incubated at 37 °C for 1 h with goat anti-mouse fluorescein isothiocyanate (FITC)-conjugated immunoglobulin G (IgG) antibody (Santa Cruz, CA, USA) diluted 1:100 in PBS (pH 7.4). Cells were washed with PBS (pH 7.4), stained with 500 nM 4′,6-diamidino-2-phenylindole (DAPI) solution for 10 min at room temperature, and washed three times with PBS (pH 8.0). Slides were mounted using SlowFade Gold antifade reagent (Invitrogen, CA, USA). Confocal fluorescence imaging was performed using a Carl Zeiss LSM 510 META confocal microscope (Carl Zeiss Inc., Jena, Germany).

2.9. Virus yield reduction assay

The TF-104 cells were infected with HRV1–3 and PRV strain at 0.01 MOI in 6-well plates. After 1 h of virus adsorption at 37 °C, the cells were washed three times with PBS and cultured in a medium containing with MeOH extract and EtOAc fraction (20–150 μg/mL) or kuraridin (6.25–50 μM) at different concentration. The untreated cell and virus controls (0.5% DMSO) were included. The supernatants were harvested after 24 h. The virus yields were determined using plaque assay for 7 days. All determinations were performed thrice in triplicate.

2.10. Statistical analysis

All experiments were repeated at least three times. The differences between groups were assessed using one-way or two-way ANOVA, followed by Tuckey post-hoc analysis. Data were

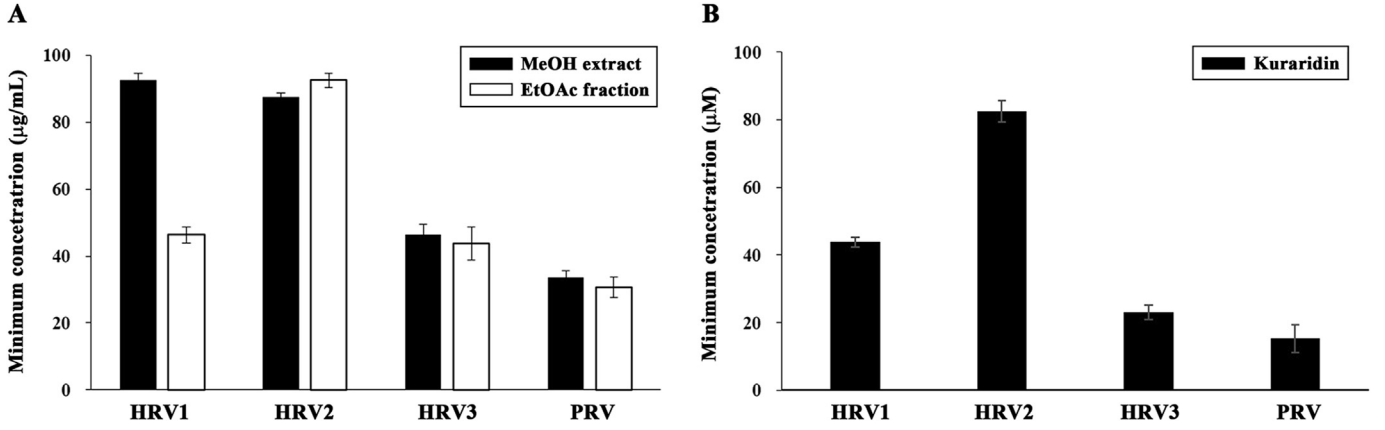

Fig. 5. Inhibitory activities of the MeOH extract, EtOAc fraction, and kuraridin on viral hemagglutination with human RBC (hRBC, type O) or bovine RBC (bRBC). Four hemagglutinating units (HAU) of HRV1–3 and PRV were mixed with an equal volume of MeOH extract, EtOAc fraction (A), kuraridin (B) or PBS (negative control) diluted two-fold, and incubated for 1 h at 4 °C. Hemagglutination activity was examined following incubation with 1% hRBC for HRV1 or 1% bRBC for HRV2–3 and PRV for 1 h at room temperature. The minimum concentrations of the extracts and kuraridin that completely inhibited viral hemagglutination were determined.

presented as mean ± ANOVA combined standard errors of the mean (S.E.M). A values of $P < 0.05$ were considered to be significant as compared to the untreated control.

3. Results

3.1. Cytotoxicity of S. flavescens extracts and kuraridin to TF-104 cells

The cell viability of TF-104 cultures treated with the two extracts and kuraridin was evaluated using the MTT assay (Fig. 3). CC_{50} (50% cytotoxic concentration) values for the MeOH extract and EtOAc fraction were 253.3 and 278.4 μg/mL, respectively, while that for kuraridin was considerably lower at 302.2 μM (Table 1). Accordingly, all experiments evaluating antiviral effects were performed at concentrations of minimal toxicity below 150 μg/mL for the MeOH extract and EtOAc fraction or 150 μM for kuraridin.

3.2. Inhibitory activity of S. flavescens on reovirus adsorption

A pre-treatment assay was performed to examine the inhibitory effect of the two extracts and kuraridin on reovirus attachment into host cells (Fig. 2A). The simultaneous treatment assay was additionally conducted to determine whether the extracts and kuraridin directly inhibit reovirus particles (Fig. 2B). In the pre-treatment assay, the MeOH extract, EtOAc fraction and kuraridin showed no inhibitory effects against HRV1–3 and PRV (data not shown). Notably, however, in the simultaneous treatment assay, two

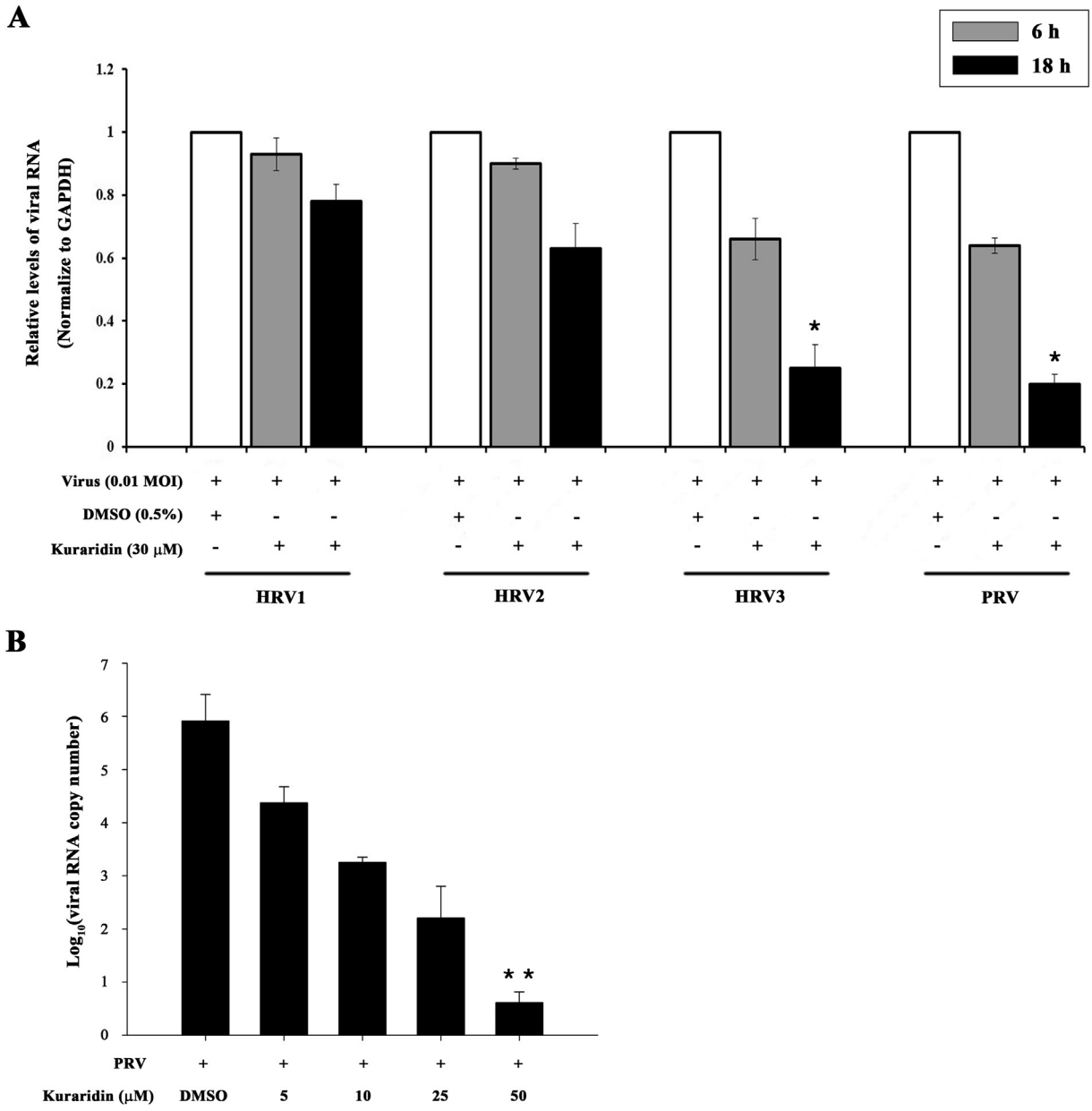

Fig. 6. Quantitative real-time PCR of reovirus viral RNA levels normalized to GAPDH. (A) TF-104 cells were infected with HRV1–3 and PRV at a MOI of 0.01. The viral inoculum was removed 1 h post-infection. TF-104 cells were treated with DMSO (0.5%) or kuraridin (30 μM). Total RNA was extracted at 6 h and 18 h post-infection, and the intracellular viral RNA levels measured. (B) TF-104 cells were infected with PRV at a MOI of 0.01. At 1 h post-infection, the inoculum was removed. Next, TF-104 cells were treated with DMSO (0.5%) or kuraridin (5, 10, 25, 50 μM). Total RNA was extracted 24 h post-infection, and the number of RNA copies of viral L1 gene measured. Data are expressed as mean ± ANOVA combined standard error of three independent replicates. $^{**}P < 0.01$, $^{*}P < 0.05$, compared to control DMSO-treated cells.

extracts inhibited reovirus entry (Fig. 4A). The MeOH extract and EtOAc fraction exhibited a decreasing order of antiviral activity against HRV3, PRV, HRV1, and HRV2, while kuraridin exhibited antiviral activity in a decreasing order against PRV, HRV3, HRV1, and HRV2 (Table 1). Interestingly, our data indicate that both the extracts and kuraridin exert stronger inhibitory effects on HRV3 and PRV than HRV1 or HRV2, with the greatest inhibitory effect of kuraridin against PRV isolated from Korean porcine diarrheic feces.

3.3. Hemagglutination inhibition (HI) activity

The simultaneous treatment assay established that either virus adsorption or cell entry is inhibited by the two extracts and kuraridin. Accordingly, we evaluated whether the extracts and kuraridin inhibit reovirus-induced hemagglutination binding of HRV1 to hRBC or HRV2–3 and PRV to bRBC. The MeOH extract and EtOAc fraction completely inhibited HRV1 attachment to hRBCs as well as HRV2–3 and PRV attachment to bRBCs at concentrations less than 92.5 μg/mL (Fig. 5), with a decreasing order of HI activity as follows: PRV, HRV3, HRV2, and HRV1 for the MeOH extract, and PRV, HRV3, HRV1, and HRV2 for the EtOAc fraction. Kuraridin exhibited a similar decreasing order of HI activity against PRV, HRV3, HRV1, and HRV2. Overall, the MeOH extract, EtOAc fraction, and kuraridin showed stronger HI activity against HRV3 and PRV than HRV1 or HRV2, consistent with the findings of the simultaneous assay. Our results clearly indicate that strong interactions of the two extracts and kuraridin with hemagglutinin on the outer-layer protein (sigma 1) of reovirus result in inhibition of viral attachment.

3.4. Antiviral activity of S. flavescens against reovirus replication

The post-treatment assay was performed to evaluate the inhibitory effects of the MeOH extract, EtOAc fraction, and kuraridin on reovirus replication (Fig. 2C). The MeOH extract and EtOAc fraction inhibited viral replication in preliminary experiments (Fig. 4B), with a decreasing order of activity against HRV3, PRV, HRV2 and HRV1 (Table 1). Kuraridin exerted decreasing antiviral activity in the following order: PRV, HRV3, HRV2, and HRV1 (Table 1). Similar to the results of the simultaneous treatment assay, all three isolate fractions showed stronger inhibitory effects on HRV3 and PRV than HRV1 or HRV2. Viral RNA levels synthesized at the early and late stages of virus infection were compared between kuraridin-treated (30 μM) and untreated infected cells. RNA extraction was performed at 6 and 18 h post-infection with HRV1–3 and PRV, and the levels of intracellular viral RNA measured via real-time PCR. Quantitative real-time PCR data disclosed reduced reovirus RNA levels in kuraridin-treated cells, compared with non-treated cells (0.5% DMSO) HRV1–3 and PRV (Fig. 6A). Viral RNA inhibition in kuraridin-treated cells was the greatest at late-stage (18 h) infection, indicating that kuraridin (30 μM) inhibits viral RNA synthesis most strongly at the late stage (18 h) than the early stage (6 h) of infection. Furthermore, we observed dose-dependent inhibition of viral RNA in PRV-infected TF-104 cells treated with 5–50 μM kuraridin for 24 h post-infection (Fig. 6B). The immunofluorescence assay conducted to investigate viral protein (sigma 1) inhibition by kuraridin (30 μM) in PRV-infected TF-104 cells demonstrated green fluorescence for virus-infected (Fig. 7B) but not mock-infected cells (Fig. 7A). Treatment of cells with kuraridin led to a marked reduction

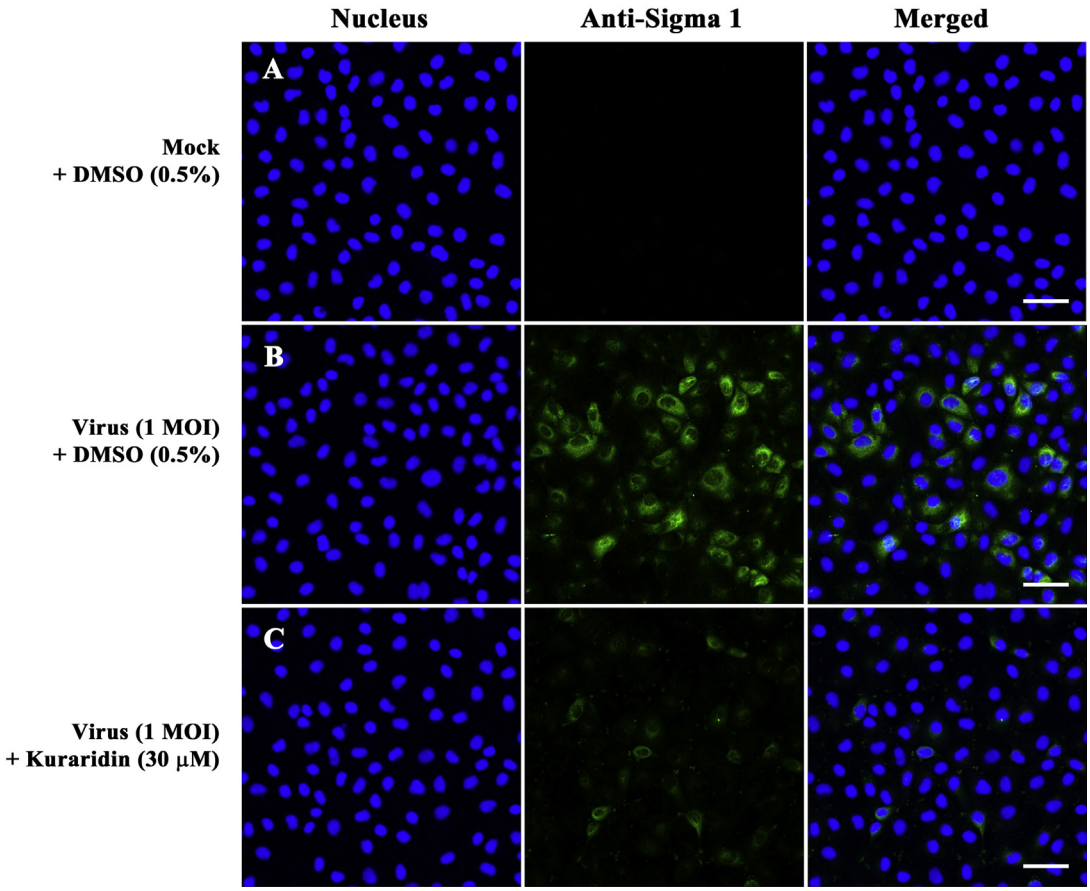

Fig. 7. Confocal fluorescence imaging of kuraridin against reovirus. TF-104 cells were mock infected (A) or infected with PRV at a MOI of 1 in the presence of DMSO (0.5%) (B) or kuraridin (30 μM) (C). After 24 h, cells were fixed in 4% paraformaldehyde. After blocking, cells were incubated with anti-sigma 1 (σ1) antibody (green). DAPI was used as the nuclear counterstain (blue). Bar = 10 μm.

in the number of fluorescent cells infected with PRV (Fig. 7C). To determine the effects of the two extracts and kuraridin on reovirus production, we performed the virus yield reduction assay. Viral yields were estimated using a plaque assay. Notably, the MeOH extract, EtOAc fraction, and kuraridin suppressed production of HRV1–3 and PRV in a dose-dependent manner indicating inhibition of reovirus shedding or release (Fig. 8).

4. Discussion

Various steps of the viral replication cycle are targets of antiviral agents, including adsorption, cell penetration, uncoating, transcription, translation, assembly and viral release from infected cells (4). We hypothesized that the antiviral effects of *S. flavescens* can be divided into two steps: 1) blockage of virus adsorption to cells and/or 2) inhibition of viral replication after cell entry. Time-of-addition experiments were performed to determine the stage at which inhibitory activities are exerted. MeOH extract, EtOAc fraction, and kuraridin of *S. flavescens* were added to TF-104 cells at three distinct time-points, specifically, prior to infection (pre-treatment), at the same time as virus infection (simultaneous) or post-infection (post-treatment) (Fig. 2).

Reovirus entry into cells is a multistep process involving several interactions between its outer layer protein (sigma 1 protein) and cell surface receptors, including sialic acid (SA) and junctional adhesion molecule-A (JAM-A) (28). The sigma 1 protein specifies tissue tropism and is responsible for hemagglutination (HA) activity and binding of SA (29, 30). The HA activity of reoviruses strongly implies a role of SA in cell binding and infectivity of reoviruses, similar to influenza A virus, rotavirus, various coronaviruses and Sendai virus (31). In the current study, the HI assay was employed to assess the inhibitory effects of the extracts and kuraridin on viral adsorption to host cells. The MeOH extract and EtOAc fraction completely inhibited HRV1 adsorption to hRBCs as well as HRV2–3 and PRV adsorption to bRBCs at concentrations below 92.5 μg/mL. Kuraridin induced complete inhibition of hemagglutination activity of HRV1 with hRBCs and HRV2–3 and PRV with bRBCs at concentrations below 82.5 μM (Fig. 5). I21nterestingly, the HI activity of kuraridin was stronger for HRV3 and PRV than HRV1 and HRV2. These differences are linked to sigma 1 protein sequences and possibly attributable to serotype-specific interactions of viral proteins with different cell surface receptors. Five residues (Asn198, Arg202, Leu203, Pro204, and Gly205) in sigma 1 protein are reported to play a role in reovirus and SA interactions (32). Additionally, SA binding by sigma 1 protein of type 3 reovirus is mediated by an eight-stranded cross β-sheet of only the T(iii) domain (residues 175–234) and hemagglutination by type 1 reovirus mediated by the T(iii) and T(iv) domains (residues 248–314) (33). Thus, the diversity of sigma 1 protein according to type 1–3

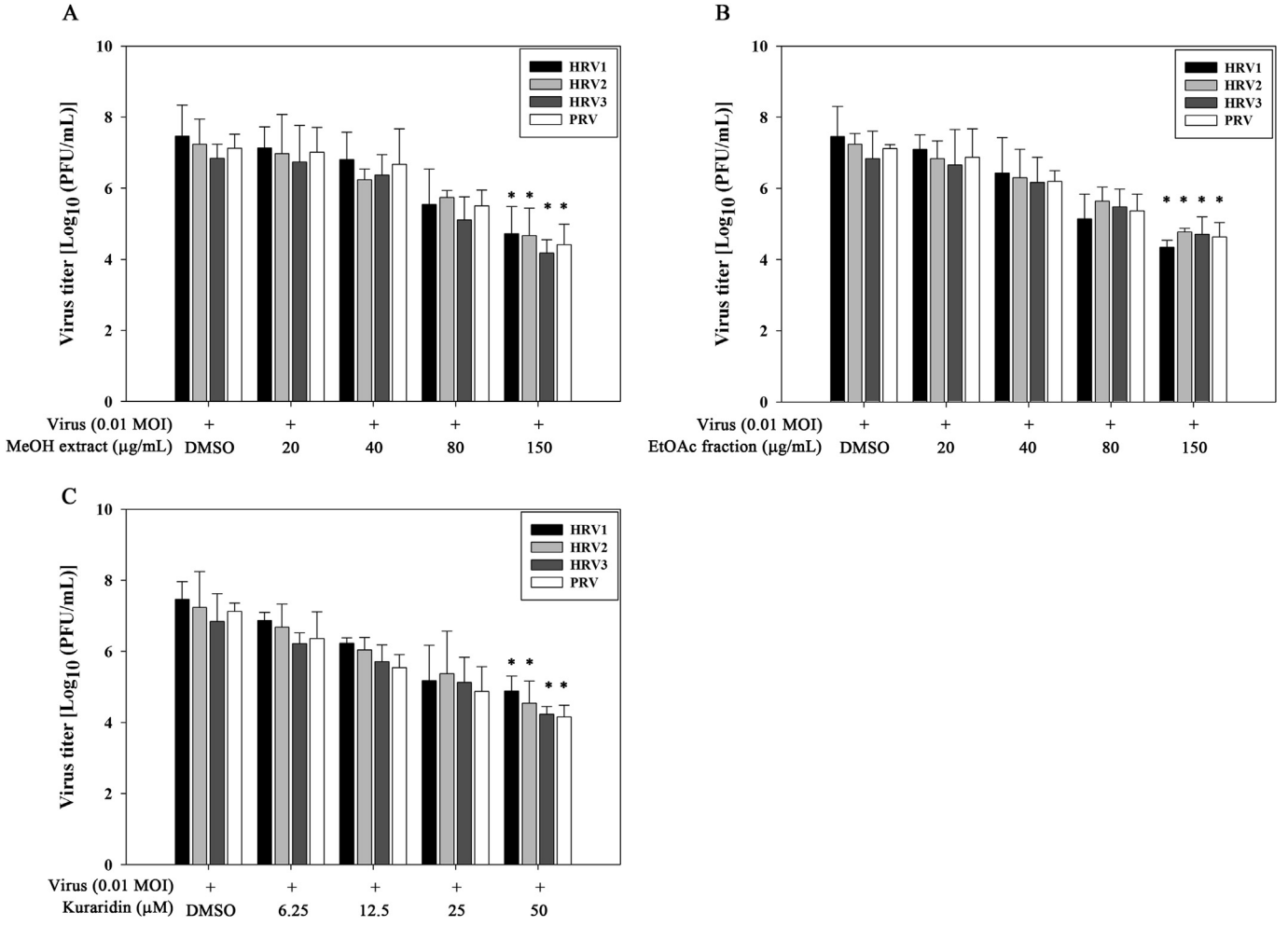

Fig. 8. Reduction of reovirus production by the MeOH extract, EtOAc fraction, and kuraridin. TF-104 cells were infected with HRV1–3 and PRV at MOI of 0.01, and treated with DMSO (0.5%), MeOH extract (20–150 μg/mL) (A), EtOAc fraction (20–150 μg/mL) (B) or kuraridin (6.25–50 μM) (C). After 24 h, supernatant fractions were harvested and virus titers determined with the plaque assay. Data are expressed as mean ± ANOVA combined standard error of three independent assays. *$P < 0.05$ compared to DMSO-treated cells that were used as control.

serotypes may influence interactions of kuraridin with hemagglutinin on the protein. HI assay results were in agreement with those of the simultaneous treatment assay (Table 1), indicating that the extracts and kuraridin potentially exert anti-reoviral activity via blockage of viral attachment to SA at the host cell surface. Inhibition of virus attachment, in turn, prevents virus entry, replication and occurrence of infection.

The extracts and kuraridin significantly inhibited reovirus replication after infection in a dose-dependent manner in the post-treatment assay (Fig. 4B). Although the mechanisms by which kuraridin inhibits reovirus replication are currently unclear, the compound is known to affect viral factors, such as RNA and protein. Our experiments showed that viral RNA levels are significantly lowered by kuraridin. Interestingly, reoviral RNA synthesis was significantly inhibited by kuraridin at the late stage (18 h) of the viral replication cycle for HRV3 and PRV (Fig. 6A). The reovirus replication cycle comprises two distinct transcription phases (primary and secondary), which occur at early and late stages, respectively. For primary transcription, viral RNA rapidly replicates at 6–8 h post-infection within progeny viral particles. Secondary transcription is mediated by particles assembled from the newly synthesized RNA and protein molecules, and mature virions are produced at >12 h post-infection (4). Our findings indicate that kuraridin inhibits viral protein synthesis (sigma 1) to produce the same changes in viral RNA levels and reduces virus shedding (Figs. 7 and 8). Based on these results, we suggest that the kuraridin suppresses reovirus replication via inhibition of viral RNA, protein synthesis and virus release.

Ribavirin is reported to exert anti-reovirus activity, inhibiting viral multiplication (34). A number of natural products have been extensively investigated for their antiviral and virucidal activities (35–39). Gallate derivatives that display antiviral effects are used as antioxidant food additives, including E−310 (propyl gallate), E−311 (octyl gallate), and E−312 (lauryl gallate) (39). Mycophenolic acid has additionally been identified as an anti-reoviral agent, acting as a reversible inhibitor of eukaryotic IMP dehydrogenase (IMPDH) (40). Another study demonstrated that chestnut and quebracho wood extracts containing tannin show antiviral activity against avian reovirus and metapneumovirus (41). The dipeptide, benzyloxycarbonyl-Phe-Ala-fluoromethyl ketone (Z-FA-FMK), is a novel potent inhibitor of reovirus pathogenesis and oncolysis *in vivo* (42). These drugs act by inhibiting reovirus replication and adsorption, but their potential side-effects are yet to be clinically evaluated. These natural products may be ideal candidates, since they are less toxic, more effective, have fewer side-effects, and are less expensive than commercially available anti-reovirus agents. The results from the current study collectively indicate that compounds isolated from *S. flavescens* may be superior to anti-reovirus agents, and further highlight the medical importance of identifying effective natural antiviral agents.

Conflict of interest

None.

Acknowledgements

This research was supported by a grant from the KRIBB Research Initiative Program, Republic of Korea.

References

(1) Sabin AB. Reoviruses. A new group of respiratory and enteric viruses formerly classified as ECHO type 10 is described. Science. 1959;130:1387–1389.
(2) Kohl C, Lesnik R, Brinkmann A, Ebinger A, Radonić A, Nitsche A, et al. Isolation and characterization of three mammalian orthoreoviruses from European bats. PLoS One. 2012;7:e43106.
(3) Tyler KL. Pathogenesis of reovirus infections of the central nervous system. Curr Top Microbiol Immunol. 1998;233:93–124.
(4) Schiff LA, Nibert ML, Tyler KL. Orthoreoviruses and their replication. In: Knipe DM, Howley PM, editors. Fields Virology. fifth ed., Vol. 2. Philadelphia: Lippincott Williams & Wilkins Press; 2007. p. 1853–1915.
(5) Tyler KL, Barton ES, Ibach ML, Robinson C, Campbell JA, O'Donnell SM, et al. Isolation and molecular characterization of a novel type 3 reovirus from a child with meningitis. J Infect Dis. 2004;189:1664–1675.
(6) Johansson PJ, Sveger T, Ahlfors K, Ekstrand J, Svensson L. Reovirus type 1 associated with meningitis. Scand J Infect Dis. 1996;28:117–120.
(7) Jassim SA, Naji MA. Novel antiviral agents: a medicinal plant perspective. J Appl Microbiol. 2003;95:412–427.
(8) Mukhtar M, Arshad M, Ahmad M, Pomerantz RJ, Wigdahl B, Parveen Z. Antiviral potentials of medicinal plant. Virus Res. 2008;131:111–120.
(9) Cecilia P, Thomas E. Antiviral medicinal herbs and phytochemicals. J Phcog. 2012;3:45–48.
(10) Leyssen P, De Clercq E, Neyts J. Molecular strategies to inhibit the replication of RNA viruses. Antivir Res. 2008;78:9–25.
(11) Zheng Y, Yao J, Shao X, Muralee N. Study on bio-active compounds from *Sophora flavescens* Ait. Nongyaoxue Xuebao. 1999;1:91–93.
(12) Li S, Lu AP, Wang YY, Li YD. Suppressive effects of a Chinese herbal medicine qing-luo-yin extract on the angiogenesis of collagen-induced arthritis in rats. Am J Chin Med. 2003;31:713–720.
(13) Zhou H, Lutterodt H, Cheng Z, Yu LL. Anti-Inflammatory and antiproliferative activities of trifolirhizin, a flavonoid from *Sophora flavescens* roots. J Agric Food Chem. 2009;57:4580–4585.
(14) Kuroyanagi M, Arakawa T, Hirayama Y, Hayashi T. Antibacterial and anti-androgen flavonoids from *Sophora flavescens*. J Nat Prod. 1999;62:1595–1599.
(15) Kang TH, Jeong SJ, Ko WG, Kim NY, Lee BH, Inagaki M, et al. Cytotoxic lavandulyl flavonones from *Sophora flavescens*. J Nat Prod. 2000;63:680–681.
(16) Kim DW, Chi YS, Son KH, Chang HW, Kim JS, Kang SS, et al. Effects of sophoraflavanone G, a prenylated flavonoid from *Sophora flavescens*, on cyclooxygenase-2 and in vivo inflammatory response. Arch Pharm Res. 2002;25:329–335.
(17) Cha JD, Moon SE, Kim JY, Jung EK, Lee YS. Antibacterial activity of sophoraflavanone G isolated from the roots of *Sophora flavescens* against methicillin–resistant *Staphylococcus aureus*. Phytother Res. 2009;23:1326–1331.
(18) Ryu YB, Curtis-Long MJ, Kim JH, Jeong SH, Yang MS, Lee KW, et al. Pterocarpans and flavanones from Sophora flavescens displaying potent neuraminidase inhibition. Bioorg Med Chem Lett. 2008;18:6046–6049.
(19) Sun M, Han J, Duan J, Cui Y, Wang T, Zhang W, et al. Novel antitumor activities of Kushen flavonoids in vitro and in vivo. Phytother Res. 2007;21:269–277.
(20) Hong-Li S, Lei L, Lei S, Dan Z, De-Li D, Guo-Fen Q, et al. Cardioprotective effects and underlying mechanisms of oxymatrine against Ischemic myocardial injuries of rats. Phytother Res. 2008;22:985–989.
(21) Liu Y, Zhang XJ, Yang CH, Fan HG. Oxymatrine protects rat brains against permanent focal ischemia and downregulates NF-kappaB expression. Brain Res. 2009;1268:174–180.
(22) Ryu SY, Lee HS, Kim YK, Kim SH. Determination of isoprenyl and lavandulyl positions of flavonoids from *Sophora flavescens* by NMR experiment. Arch Pharm Res. 1997;20:491–495.
(23) Finney DJ. In: Finney DJ, editor. Statistical Method in Biological Assay. first ed. London: Griffin; 1952. p. 661.
(24) Kwon HJ, Ryu YB, Kim YM, Song N, Kim CY, Rho MC, et al. In vitro antiviral activity of phlorotannins isolated from Ecklonia cava against porcine epidemic diarrhea coronavirus infection and hemagglutination. Bioorg Med Chem. 2013;21:4706–4713.
(25) Kwon HJ, Kim HH, Kim HJ, Park JG, Son KY, Jung J, et al. Detection and molecular characterization of porcine type 3 orthoreoviruses circulating in South Korea. Vet Microbiol. 2012;157:456–463.
(26) Iskarpatyoti JA, Morse EA, McClung RP, Ikizler M, Wetzel JD, Contractor N, et al. Serotype-specific differences in inhibition of reovirus infectivity by human-milk glycans are determined by viral attachment protein ó1. Virology. 2012;433:489–497.
(27) Douville RN, Su RC, Coombs KM, Simons FE, Hayglass KT. Reovirus serotypes elicit distinctive patterns of recall immunity in humans. J Virol. 2008;82:7515–7523.
(28) Kirchner E, Guglielmi KM, Strauss HM, Dermody TS, Stehle T. Structure of reovirus sigma 1 in complex with its receptor junctional adhesion molecule-A. PLoS Pathog. 2008;4:e1000235.
(29) Fajardo E, Shatkin AJ. Expression of the two reovirus S1 gene products in transfected mammalian cells. Virology. 1990;178:223–231.
(30) Belli BA, Samuel CE. Biosynthesis of reovirus-specified polypeptides: identification of regions of the bicistronic reovirus S1 mRNA that affect the efficiency of translation in animal cells. Virology. 1993;193:16–27.
(31) Isa P, Arias CF, López S. Role of sialic acids in rotavirus infection. Glycoconj J. 2006;23:27–37.
(32) Reiter DM, Frierson JM, Halvorson EE, Kobayashi T, Dermody TS, Stehle T. Crystal structure of reovirus attachment protein σ1 in complex with sialylated oligosaccharides. PLoS Pathog. 2011;7:e1002166.
(33) Chappell JD, Duong JL, Wright BW, Dermody TS. Identification of carbohydrate-binding domains in the attachment proteins of type 1 and type 3 reoviruses. J Virol. 2000;74:8472–8479.
(34) Rankin Jr JT, Eppes SB, Antczak JB, Joklik WK. Studies on the mechanism of the antiviral activity of ribavirin against reovirus. Virology. 1989;168:147–158.

(35) Bonn D. Green coffee beans may yield new class of anti-HIV-1 agents. Lancet. 1998;352:1039.
(36) Isaacs CE, Wen GY, Xu W, Jia JH, Rohan L, Corbo C, et al. Epigallocatechin gallate inactivates clinical isolates of herpes simplex virus. Antimicrob Agents Chemother. 2008;52:962–970.
(37) Utsunomiya H, Ichinose M, Uozaki M, Tsujimoto K, Yamasaki H, Koyama AH. Antiviral activities of coffee extracts in vitro. Food Chem Toxicol. 2008;46:1919–1924.
(38) Xu J, Wang J, Deng F, Hu Z, Wang H. Green tea extract and its major component epigallocatechin gallate inhibits hepatitis B virus in vitro. Antivir Res. 2008;78:242–249.
(39) Arakawa T, Yamasaki H, Ikeda K, Ejima D, Naito T, Koyama AH. Antiviral and virucidal activities of natural products. Curr Med Chem. 2009;16:2485–2497.
(40) Hermann LL, Coombs KM. Inhibition of reovirus by mycophenolic acid is associated with the M1 genome segment. J Virol. 2004;78:6171–6179.
(41) Lupini C, Cecchinato M, Scagliarini A, Graziani R, Catelli E. In vitro antiviral activity of chestnut and quebracho woods extracts against avian reovirus and metapneumovirus. Res Vet Sci. 2009;87:482–487.
(42) Kim M, Hansen KK, Davis L, van Marle G, Gill MJ, Fox JD, et al. Z-FA-FMK as a novel potent inhibitor of reovirus pathogenesis and oncolysis in vivo. Antivir Ther. 2010;15:897–905.

List of abbreviation

S. flavescens: Sophora flavescens
MRV: Mammalian reovirus
HRV1–3: human type 1–3 reoviruses
PRV: Korean porcine reovirus
T1L: type 1 Lang
T2J: type 2 Jones
T3D: type 3 Dearing
T4N: type 4 Ndelle
HIV: human immunodeficiency virus
HBV: hepatitis B virus
TF-104: Fetal rhesus monkey kidney
EMEM: Eagle's minimum essential medium
FBS: fetal bovine serum
ATCC: American Type Culture Collection
CPE: viral cytopathic effect
HI: hemagglutination inhibition
hRBCs: human red blood cells
bRBCs: bovine red blood cells
FITC: fluorescein isothiocyanate
DAPI: 4′,6-diamidino-2-phenylindole
CC_{50}: 50% cytotoxic concentration
EC_{50}: 50% effective inhibitory concentrations
SA: sialic acid
JAM-A: junctional adhesion molecule-A
HA: hemagglutination
IMPDH: IMP dehydrogenase
Z-FA-FMK: dipeptide, benzyloxycarbonyl-Phe-Ala-fluoromethyl ketone